TYPE Original Research
PUBLISHED 12 November 2025
DOI 10.3389/feart.2025.1679009



#### **OPEN ACCESS**

EDITED BY
Xiao-Ping Xia,
Chinese Academy of Sciences (CAS), China

#### REVIEWED BY

Madhavaraju Jayagopal, National Autonomous University of Mexico, Mexico Jingna Liu, Guilin University of Technology, China

\*CORRESPONDENCE

Tianjia Liu,

Iutianjia.syky@sinopec.com

RECEIVED 04 August 2025 REVISED 21 October 2025 ACCEPTED 24 October 2025 PUBLISHED 12 November 2025

#### CITATION

Liu T, Zhang D, Zhai Y, Liu X, Zhang L, Fan L, Cheng C and Fang S (2025) Detrital zircon population of the Middle Triassic sediments in the eastern Sichuan Basin, South China and implications for tectonic setting. Front. Earth Sci. 13:1679009. doi: 10.3389/feart.2025.1679009

#### COPYRIGHT

© 2025 Liu, Zhang, Zhai, Liu, Zhang, Fan, Cheng and Fang. This is an open-access article distributed under the terms of the Creative Commons Attribution License (CC BY). The use, distribution or reproduction in other forums is permitted, provided the original author(s) and the copyright owner(s) are credited and that the original publication in this journal is cited, in accordance with accepted academic practice. No use, distribution or reproduction is permitted which does not comply with these terms.

# Detrital zircon population of the Middle Triassic sediments in the eastern Sichuan Basin, South China and implications for tectonic setting

Tianjia Liu<sup>1</sup>\*, Dianwei Zhang<sup>1</sup>, Yonghe Zhai<sup>1</sup>, Xiangbai Liu<sup>2</sup>, Lei Zhang<sup>1</sup>, Lingxiao Fan<sup>1</sup>, Chuanjie Cheng<sup>1</sup> and Shaobo Fang<sup>3</sup>

<sup>1</sup>Petroleum Exploration and Production Research Institute, SINOPEC, Beijing, China, <sup>2</sup>Research Institute of Petroleum Exploration and Development, PetroChina, Beijing, China, <sup>3</sup>Institute of Mineral Resources, Chinese Academy of Geological Sciences, Beijing, China

The closure of the Paleo-Tethys Ocean lead to the collisional amalgamation of the various blocks including South China, Indochina and North China blocks, which results in the formation of the Qinling and Ailaoshan orogenic belts. But the tectonic evolution of the two orogenic belts remains highly debated during the Triassic. The eastern Sichuan Basin, preserving the complete Triassic depositional successions, offers crucial insight into the tectonic evolution of the two orogenic belts in this period. Detailed geological investigations and provenance analyses using detrital zircon U-Pb-Hf isotopic data and trace element compositions are conducted on the Middle Triassic Leikoupo Formation samples in the eastern Sichuan Basin. The age distribution of the middle part of the Leikoupo Formation (Member-2) shows five age clusters of 290~230 Ma, 330~290 Ma, 470~390 Ma, 900~840 Ma and 1400~1200 Ma, and those of the top (Member-3) show four age clusters of 250~238 Ma, 330~300 Ma, 960~900 Ma and 2550~2450 Ma. Considering proximity and widespread distribution, the sediments of the sample at middle part are interpreted to source from the Ailaoshan orogenic belt, the North Qinling orogenic belt and late Paleozoic granites in the Cathaysian Block. The samples at the top primarily originated from the Ailaoshan orogenic belt, basement rocks and Neoproterozoic granites in the Yangtze Block and late Paleozoic granites in the Cathaysian Block. Provenance analysis indicates that the North Qinling orogenic belt can provide a large amount of materials for the Middle Triassic, which suggests this belt was in an uplift stage and was the extension of the Caledonian orogeny since the early Paleozoic. Combining the obtained ages, published data and lithofacies paleogeography, the Early-Middle Triassic source rocks have contributions from the early Mesozoic granites in Ailaoshan orogenic belt, which suggests the Ailaoshan orogenic belt has experienced initial tectonic uplift in the Early Triassic. This initial uplift is related to the collisional amalgamation between the South China Block and Indochina Block.

KEYWORDS

detrital zircons, provenance, tectonic evolution, Leikoupo formation, Qinling and Ailaoshan orogenic belts

#### 1 Introduction

The collisional amalgamation of various blocks including South China, Indochina and North China blocks driven by the closure of the Paleo-Tethys Ocean results in the formation of the Qinling and Ailaoshan orogenic belts (Figure 1; Liu et al., 2023). Due to intense tectonic metamorphic deformation events during the Cenozoic, much geological evidence has been completely altered or eroded, thereby complicating the interpretation of the Triassic tectonic history of the Qinling and Ailaoshan orogenic belts. The debate over the uplift history of the Qinling orogenic belt (QOB) has persisted for decades and is focused on two contentious points: (1) Previous studies suggest that this belt underwent extensive uplift in the Indosinian stage (Zhang et al., 1996; Chen, 2010). (2) Several scholars have pointed out that this belt underwent long term multistage tectonic evolution, with the uplift process primarily controlled by the Caledonian orogenic movement and Indosinian orogenic movement (Ren et al., 2019). Furthermore, the initial tectonic uplift of the Ailaoshan orogenic belt (AOB) related to the collisional amalgamation between the South China Block (SCB) and Indochina Block (ICB) remains highly debated with the ages spanning the Late Permian to the Late Triassic (Yunnan Bureau of Geology and Mineral Resources, 1990; Wang et al., 2020). Therefore, further discussion is needed to resolve this dispute and gains a deeper understanding to reconstruct the tectonic evolution of the QOB and AOB in the Triassic.

In an orogenic belt-basin system, debris within the basin frequently preserves a large amount of geological information connected to the evolution of the belt, and enables the reconstruction of evolution of the belt through debris (Cawood et al., 2012; Caracciolo, 2020; Wang et al., 2023). Zircons have extremely physical and chemical stability and are not easily affected by weathering, transportation, deposition, and erosion, which retain the original information of their source rocks (Fedo et al., 2003; Siebel et al., 2009; Gehrels, 2014; Ramírez-Montoya et al., 2022; Jian et al., 2024). U-Pb detrital zircon geochronology in sediments can be used to discriminate source terranes and estimate the uplift or non-uplift state of the orogenic belt (Gehrels, 2014; Terentiev and Santosh, 2016; Madhavaraju et al., 2019; González-León et al., 2020; Galindo-Ruiz et al., 2025; Ramirez-Montoya et al., 2025).

In this paper, we collected samples from the Middle Triassic Leikoupo Formation sediments in the Dabazi section, eastern Sichuan Basin. By using detrital zircon U–Pb–Hf isotopic data and trace element compositions, the potential sources were discussed. This study seeks to reconstruct the tectonic history of the Qinling and Ailaoshan orogenic belts during the Middle Triassic through provenance analysis.

## 2 Geological setting

#### 2.1 Qinling orogenic belt

The QOB is a tectonic domain between the North China Block (NCB) and the SCB, and is adjacent to the Kunlun–Qilian orogenic belt to the west and the Dabie–Sulu orogenic belt to the east (Dong et al., 2013). This belt experienced multi-stage complex

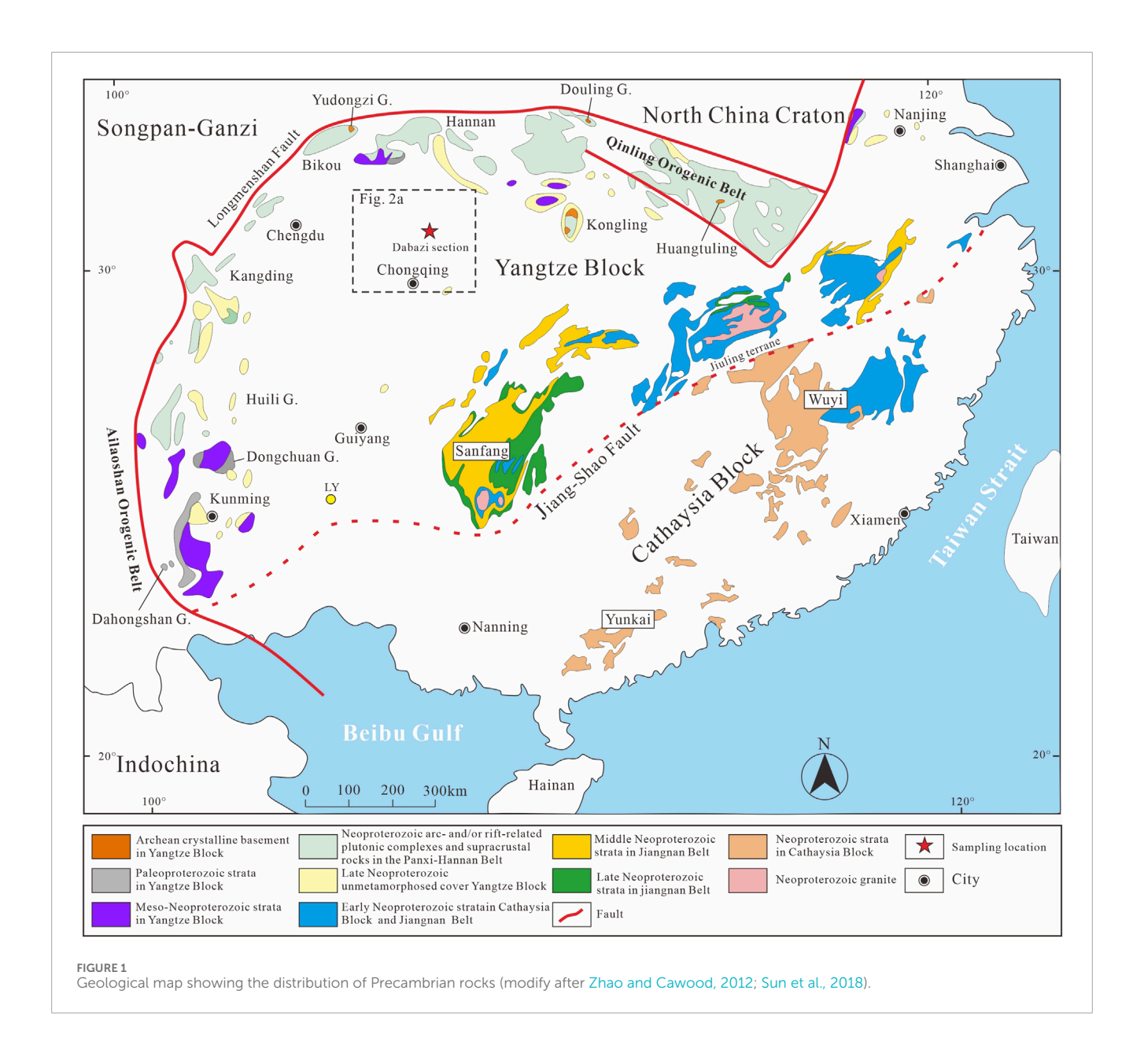
tectonic evolution (Zhang et al., 1996; 2001), and was formed by the Middle-Late Triassic eventual collision between the NCB and SCB. This belt subsequently entered Early Jurassic to Early Cretaceous innercontinental orogenic stage (Dong et al., 2013; 2022; Dong and Santosh, 2016). It could be split into two structurally tectonic units: North Qinling orogenic belt (NQOB) and South Qinling orogenic belt (SQOB) (Zhang et al., 2001). The NQOB is located between the Luonan-Luanchuan-Fangcheng fault and the Shangdan suture zone. It consists of Precambrian basement, Neoproterozoic and early Paleozoic ophiolites and volcanic-sedimentary sequences, which are unconformably overlain by Carboniferous-Permian sedimentary successions (Dong et al., 2011). The SQOB is located between the Shangdan suture zone and the Mianlue suture zone and is characterized by a south-vergent imbricated thrust-fold (Zhang et al., 2001). It mostly consists of Neoarchean basement, Neoproterozoic volcano-sedimentary sequences, and Sinian to Middle Triassic sedimentary successions (Dong and Santosh, 2016). During the Neoproterozoic to early Paleozoic, the NQOB had tectonic affinity with the southern margin of the NCB. The northward underthrusting of the Shangdan Ocean caused the NQOB to become an active plate margin in the Cambrian. Then, the NQOB and SQOB underwent tectonic convergence along the Shangdan suture zone in the middle Paleozoic. The Early Paleozoic spreading of the Mianlue Ocean resulted in the separation of the SQOB from the SCB in the early Paleozoic. The subsequent collision between the South and North China blocks culminated in the formation of the QOB (Dong and Santosh, 2016).

#### 2.2 Ailaoshan orogenic belt

The AOB is an NW-SE trending tectonic unit and located west of the SCB, which extends over 400 km with an average width of 60 km (Figure 1). Three major fault zones are distributed within this tectonic belt, from northeast to southwest: the Ailaoshan fault zone, Tengtiaohe fault zone, and Jiujia-Anding fault zone (Yunnan Bureau of Geology and Mineral Resources, 1990). This belt has experienced a long history of tectonic evolution, including Devonian featuring continental rifting, early Carboniferous-middle Permian seafloor spreading, late Permian oceanic lithosphere underthrusting, Late Triassic-Cenozoic continent-continent collision, and Cenozoic left-lateral shearing (Zhong, 1998). This belt mainly consists Paleo- and Mesoproterozoic metamorphic rocks (amphibolite rock, granulite rock and greenschist), Paleozoic-Mesozoic sedimentary and Permian-Traissic igneous rocks.

#### 2.3 Study region and samples

The Sichuan Basin is located in the western margin of the SCB (Figure 1a) and covers an area of  $1.8 \times 10^5$  km². It is bounded by the QOB to the northeast, the Longmenshan to the northwest and close to the AOB to the southwest (He et al., 2020). The Sinian to Middle Triassic marine carbonate rocks in the basin have a thickness of  $4100 \sim 7000$  m, and the Upper Triassic to the Quaternary continental clastic rocks have a thickness of  $3500 \sim 6000$  m. This basin comprises five secondary tectonic units: northern gentle structural zone, the

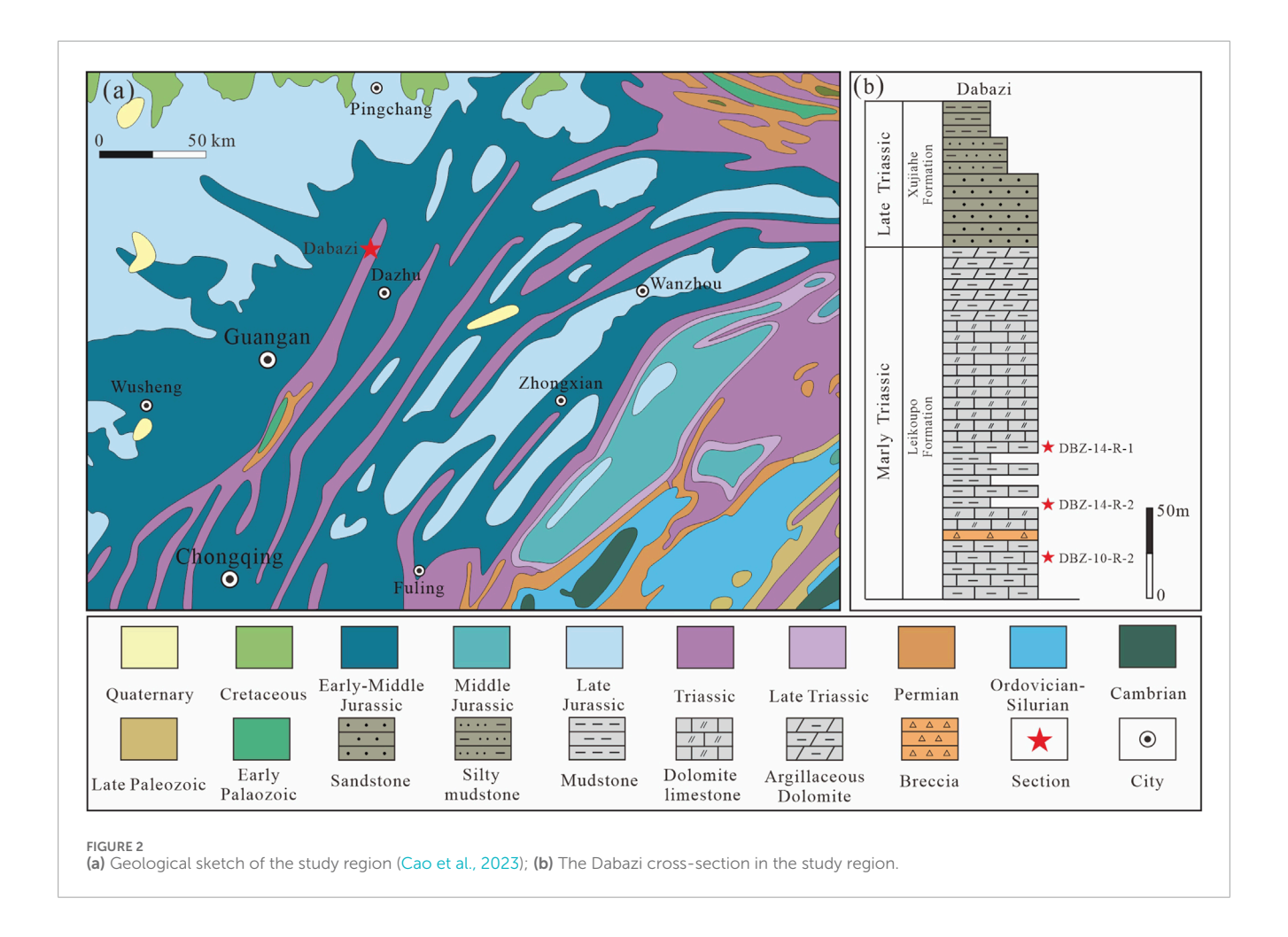


western depression, southern low-steep structural zone, the central uplift and the eastern steep structural zone.

The Middle-Late Triassic stratigraphic successions are well distributed in the study region (Figure 2a). The Leikoupo Formation mainly preserves continuous carbonate depositional from the underlying Early Triassic Jialingjiang Formation, with an unconformity surface separating from the overlying Late Triassic Xujiahe Formation. During the deposition of Leikoupo Formation, it suffered from remarkable changes with further marine regression due to tectonic uplift, which made the deposits of gypsum rock sedimentation. The sedimentary environment of the study region was restricted to an evaporitic platform during the Leikoupo period. This formation features multiple layers of marine carbonate and evaporite, including limestone, dolomite, gypsum and shale, and could be subdivided into three members: Member-1 comprises dolomite, micrite, breccia, and gypsum with a thickness of ~150 m, which conformably overlies the "mung bean

rock" bed; Member-2 includes dolomitic mudstone, argillaceous dolomite and argillaceous limestone with a thickness of ~120 m; Member-3 inherited the sedimentary model of Member-2 and was composed of up to 350 m of dolomite limestone, argillaceous dolomite, calcareous mudstone and argillaceous limestone. The study region underwent tectonic uplift due to the Indosinian movement, and the Member-4 was partially exposed to the surface and experienced denudation (He et al., 2020).

The Dabazhai section (DBZ) is studied in Pingba village, Quxian County, Dazhou city, eastern Sichuan (30°56′53.07″N, 107°9′47.91″E), and we collected three representative samples from the Middle Triassic Leikoupo Formation (Figure 2b). The sampling interval in the section is typically interbedded with argillaceous limestone and mudstone, with mud content downwardly increasing. Among them, sample DBZ-10-R-1 is collected from the dark grey middle-bedded mudstone at the Member-2 (Figures 3a,b; Figures 4a,b); sample DBZ-14-R-1 and DBZ-14-R-2 are collected



from the grayish yellow thick and middle-bedded argillaceous limestone at the Member-3 (Figures 3c-f; Figures 4c-f). These samples exhibit high content of clay minerals, with a content greater than 25%.

## 3 Analytical methods

Zircon separation is through standard heavy-liquid separation and magnetic method at Hongchuang GeoAnalysis, Nanjing. After the samples were crushed and pulverized to 40–60 mesh, zircons were separated by using conventional magnetic and heavy-liquid methods, and then hand-picked under binocular microscope. Approximately 300 grains for each sample were mounted in epoxy and polished to expose the maximum section (1/2) of zircon crystals. Zircon grains were photographed in transmitted light and reflected light, and then imaged by cathodoluminescence (CL) to reveal their morphology and internal textures of zircon grains.

Zircon U–Pb isotope and trace element analyses were conducted at the Institute of Mineral Resources, Chinese Academy of Geological Sciences. The Finnigan Neptune ICP-MS and a Newwave UP 213 Laser-Ablation system were used for the analysis. The detailed analytical technique was detailed by Liu et al. (2010). The diameter of the zircon beam spot was 25  $\mu$ m, and the repetition

rate was 10 Hz. Every set of ten sample analyses was followed by analysis of zircon standards GJ-1, SRM610 and 91500. Zircon 91500 was used as an external standard to correct <sup>207</sup>Pb/<sup>206</sup>Pb, <sup>206</sup>Pb/<sup>238</sup>U, <sup>207</sup>Pb/<sup>235</sup>U and <sup>208</sup>Pb/<sup>232</sup>Th ratios. Data processing was performed with ICPMSDataCal software, and age calculations and concordia diagrams were completed with the ISOPLOT program. Zircon ages were taken as <sup>207</sup>Pb/<sup>206</sup>Pb ages for grains older than 1000 Ma and <sup>206</sup>Pb/<sup>238</sup>U ages for grains younger than 1000 Ma.

In situ Lu–Hf isotopic analyses were conducted using a Neptune Plus MC-ICP-MS equipped with a 193 nm laser ablation system. The spot size was 32  $\mu$ m, and the repetition rate was 8 Hz with helium used as the carrier gas. GJ1 was used as the reference material. Spots for Hf isotope analysis and spots for U–Pb dating analysis were incompletely coincident, and they were all in the same zircon grains. Operating circumstances and procedures refer to Hou et al. (2007).

#### 4 Results

#### 4.1 Detrital zircon U-Pb dating

A total of 310 zircon grains from samples were subjected to U-Pb geochronological analysis. Among them, 194 grains

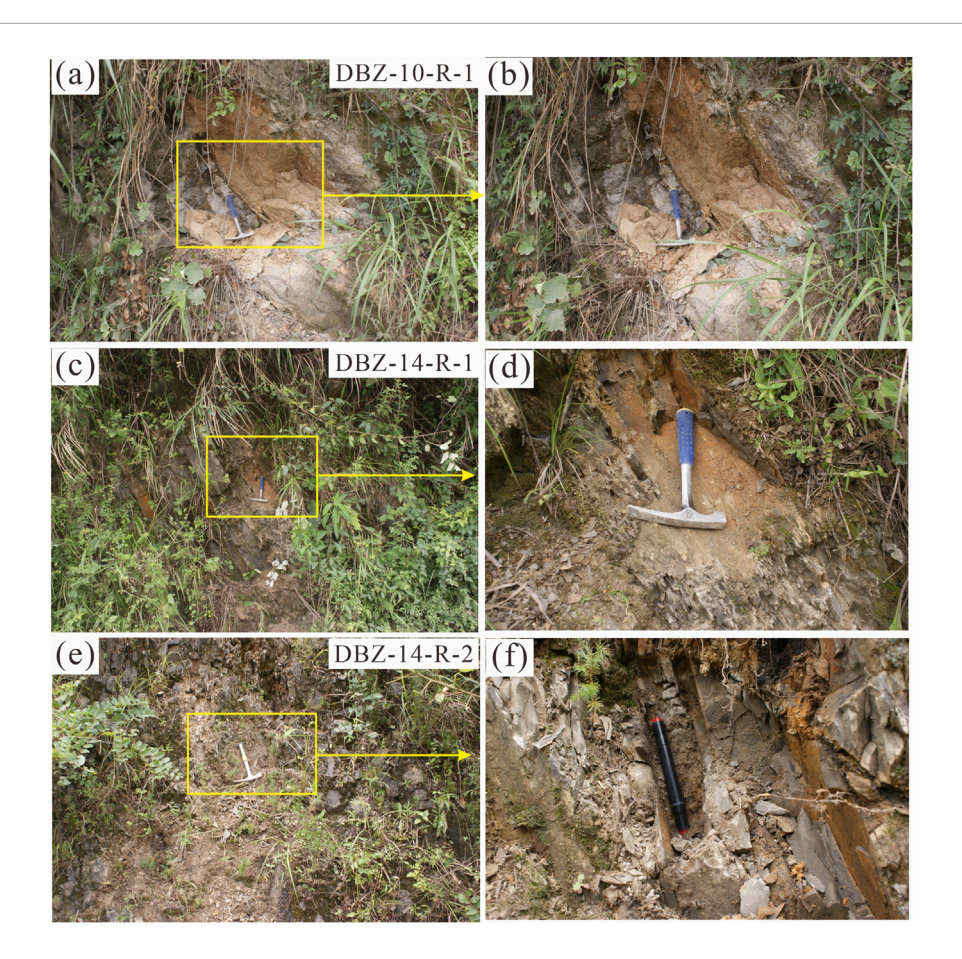


FIGURE 3
Field photographs showing the sampling locations. (a,b) mudstone at the middle of the Leikoupo Formation; (c,d) argillaceous limestone at the top of the Leikoupo Formation; (e,f) argillaceous limestone at the top of the Leikoupo Formation.

with >90% concordance are selected for final interpretation. The complete data can be found in Supplementary Table S1. The cathodoluminescence images indicate that zircon grains of samples have euhedral to subhedral shapes and measures between 80 and 150  $\mu m$  in length. Most zircon grains exhibit well-preserved oscillatory zoning, consistent with a magmatic zircon (Figure 5).

The sample DBZ-10-R-1 produced 120 U-Pb isotopic analyses, and a total of 54 analyses yielded scattered ages of 2509~239 Ma. The age population can be divided into five clusters at 250~238 Ma, 330~290 Ma, 470~390 Ma, 900~840 Ma and 1400~1200 Ma with main peaks at 242 Ma, 309 Ma, 403 Ma, 863 Ma and 1300 Ma (Figures 6a,b).

The sample DBZ-14-R-1 produced a total of 100 U-Pb isotopic analyses, and a total of 75 analysesy ielded scattered ages of 3208~234 Ma. The age spectra can be divided into two clusters at 290~234 Ma and 450~400 Ma with main peaks at 240 Ma and 418 Ma (Figures 6c,d).

The sample DBZ-14-R-2 produced a total of 90 U-Pb isotopic analyses, and a total of 65 analyses yielded scattered ages of 3000~238 Ma. The age spectra can be divided into four clusters at 250~238 Ma, 330~300 Ma, 960~900 Ma, and 2550~2450 Ma with main peaks at 245 Ma, 318 Ma, 933 Ma and 2506 Ma (Figures 6e,f).

# 4.2 Detrital zircon trace element compositions

The geochemical composition of the detrital zircon is detailed in the Supplementary Table S2. Most zircons display Th/U ratios exceeding 0.1 (Figures 7a,c,e), suggesting a magmatic origin. The REE pattern of these zircon grains is enriched in heavy REEs, accompanied by positive Ce anomalies and negative Eu anomalies (Figures 7b,d,f). The detrital zircons primarily fall within the continental zircon fields in the Hf-U/Yb and Y-U/Yb diagrams (Figures 8a,b), and dominantly fall within the arc-related/orogenic field in the Th/U-Nb/Hf and Th/Nb-Hf/Th diagrams (Figures 8c,d).

#### 4.3 Detrital zircon Hf isotope compositions

A total of 31 dated zircons were further analyzed for Lu-Hf isotopic analyses: 14 zircons for sample DBZ-14-R-1, 17 zircons for sample DBZ-14-R-2. The zircons Lu-Hf isotopic data is rendered in the Supplementary Table S3; Figure 9.

The zircon grains of DBZ-14-R-1 in the age group with a peak at 240 Ma have  $^{176}$ Hf/ $^{177}$ Hf ratios within the range of 0.282321 $\sim$ 0.282755,  $\epsilon$ Hf(t) values within the range of  $-10.9\sim+4.5$ 

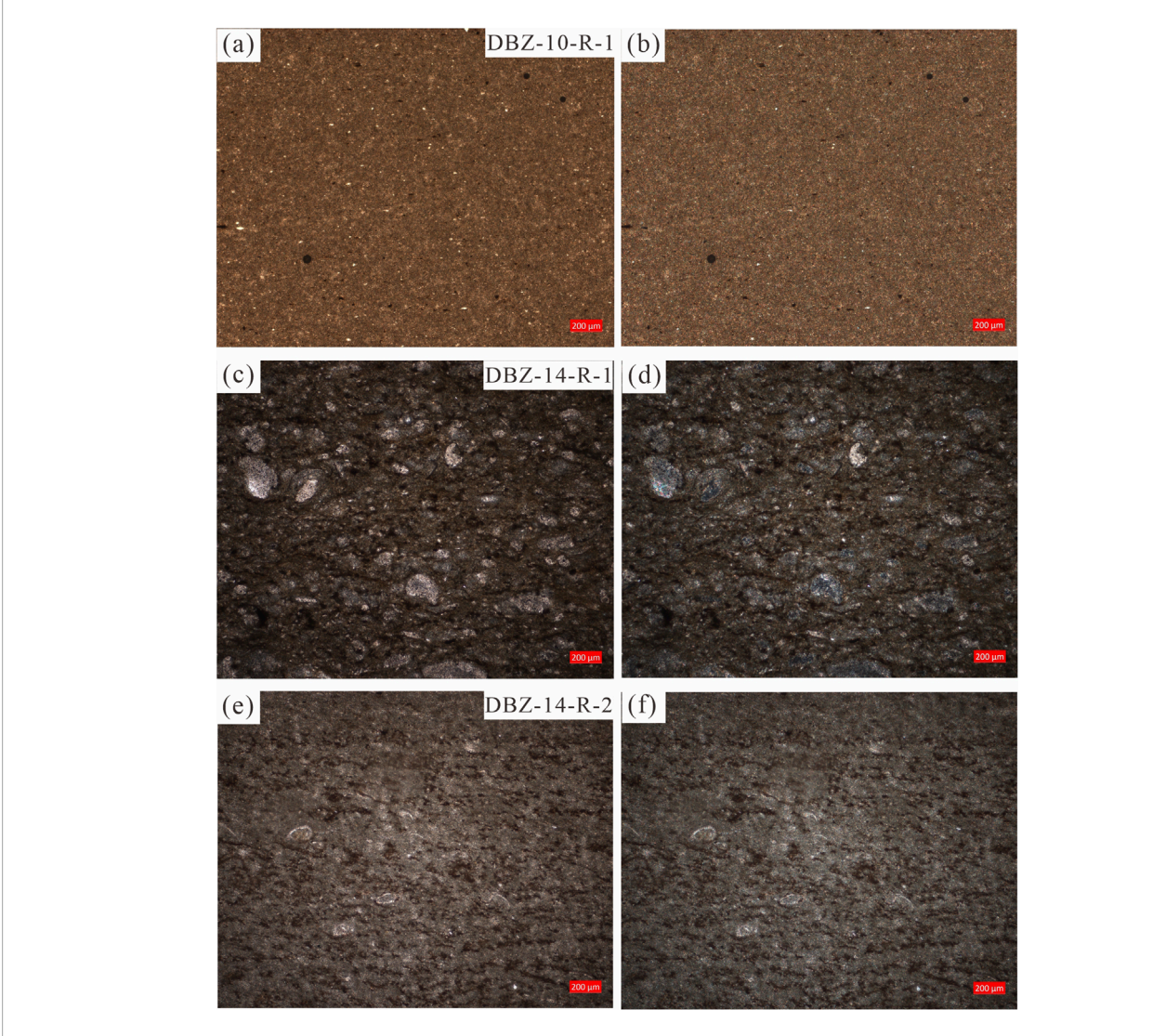


FIGURE 4 Photomicrographs of the samples in the study region. (a,b) DBZ-10-R-1. (c,d) DBZ-14-R-1. (e,f) DBZ-14-R-2.

with an average of 1.1, and two-stage model ( $\rm T_{\rm DM2})$  ages within the range of 983~1952 Ma.

The zircon grains of DBZ-14-R-2 in the age group with a peak at 245 Ma have  $^{176} Hf/^{177} Hf$  ratios within the range of 0.282370~0.282377,  $\epsilon Hf(t)$  values within the range of -9.0~-8.8, and  $T_{\rm DM2}$  ages within the range of 1832~1827 Ma; the zircon grains in the age peak at 933 Ma have  $^{176} Hf/^{177} Hf$  ratios within the range of 0.282021~0.282507,  $\epsilon Hf(t)$  values within the range of -6.6~11, and  $T_{\rm DM2}$  ages within the range of 2201~1117 Ma; the zircon grains in the age peak at 2506 Ma have  $^{176} Hf/^{177} Hf$  ratios within the range of 0.281175~0.281304,  $\epsilon Hf(t)$  values within the range of -2.7~3.3, and  $T_{\rm DM2}$  ages within the range of 3184~2816 Ma.

## 5 Discussion

# 5.1 Sedimentary provenance of Leikoupo Formation

The three samples yield a multi-peak distribution pattern of zircons, and can be divided into six major age groups of 290~234 Ma, 330~290 Ma, 470~390 Ma, 960~840 Ma, 1400–1200 Ma, and 2550~2450 Ma. This indicates that the samples have potential sources from Archean, Paleoproterozoic, Mesoproterozoic, Neoproterozoic, Paleozoic and early Mesozoic rock units.

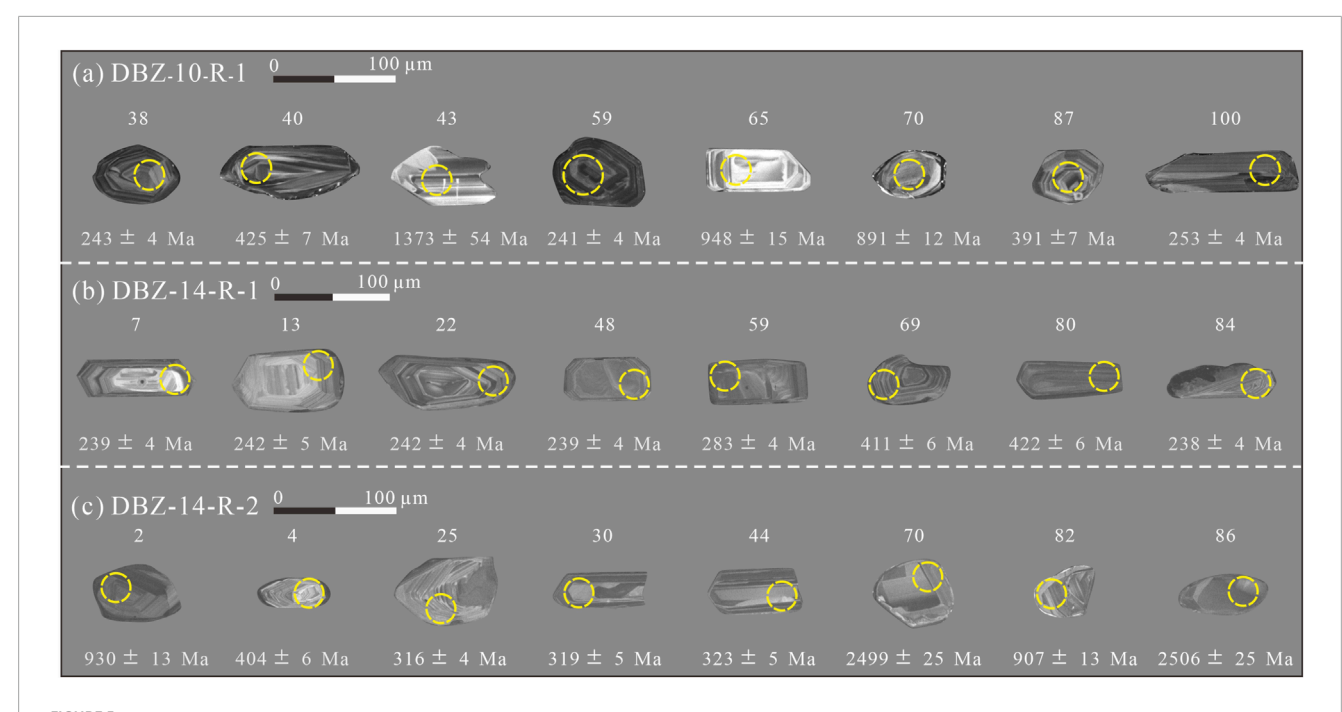


FIGURE 5
Representative cathodoluminescence (CL) images of representative zircon grains from samples and their U–Pb ages and  $\varepsilon_{\rm Hf(t)}$  values. The white and black circles represent the analytical sites of the zircon Hf isotope. (a) DBZ-10-R-1. (b) DBZ-14-R-2. (c) DBZ-14-R-2.

# 5.1.1 Archean to early proterozoic zircons (2550~2450 Ma)

Sample DBZ-14-R-2 contains detrital zircon age peak in the late Archean to early Proterozoic. However, this age population does not constitute the dominant age peak in other two samples. The zircon ages of 2600~2400 Ma are main constituent part, with mostly positive  $\varepsilon Hf(t)$  values of  $-2.7 \sim +3.3$ . These ages are coincident with the period of global continental crustal growth of the Yangtze Block (Yao et al., 2011). The Yangtze Block is distinguished by the deposits of Neoarchean-early Paleoproterozoic crystalline basement rocks, which are confined in the margins of the block. Previous researches have documented magmatism at 2.8~2.5 Ga (Zheng et al., 2006; Chen et al., 2013; Guo et al., 2015), zircons from the Douling Complex yields the age of ~2.5 Ga (Wu et al., 2014), and the Yudongzi Complex records magmatic events at 2.8~2.4 Ga (Zhou et al., 2018; Hui et al., 2017; 2019; Chen et al., 2019). The EHf(t) values of these rock units in the Yangtze Block have a characteristic with positive to negative values (Hu et al., 2013).

#### 5.1.2 Mesoproterozoic zircons (1400~1200 Ma)

The Mesoproterozoic zircons (1400~1200 Ma) play a significant role in only sample DBZ-10-R-1 with an age population centered at 1300 Ma. The sporadic occurrence of igneous rocks at approximately 1350 Ma in the NQOB, includes the Danfeng gneiss yields an age of 1350 Ma (Yang et al., 2010) and Wuguan amphibolite yields an age of 1382 Ma (Pei et al., 1997), which are the major parent rock for the Mesoproterozoic zircon grains in the samples.

#### 5.1.3 Neoproterozoic zircons (960~840 Ma)

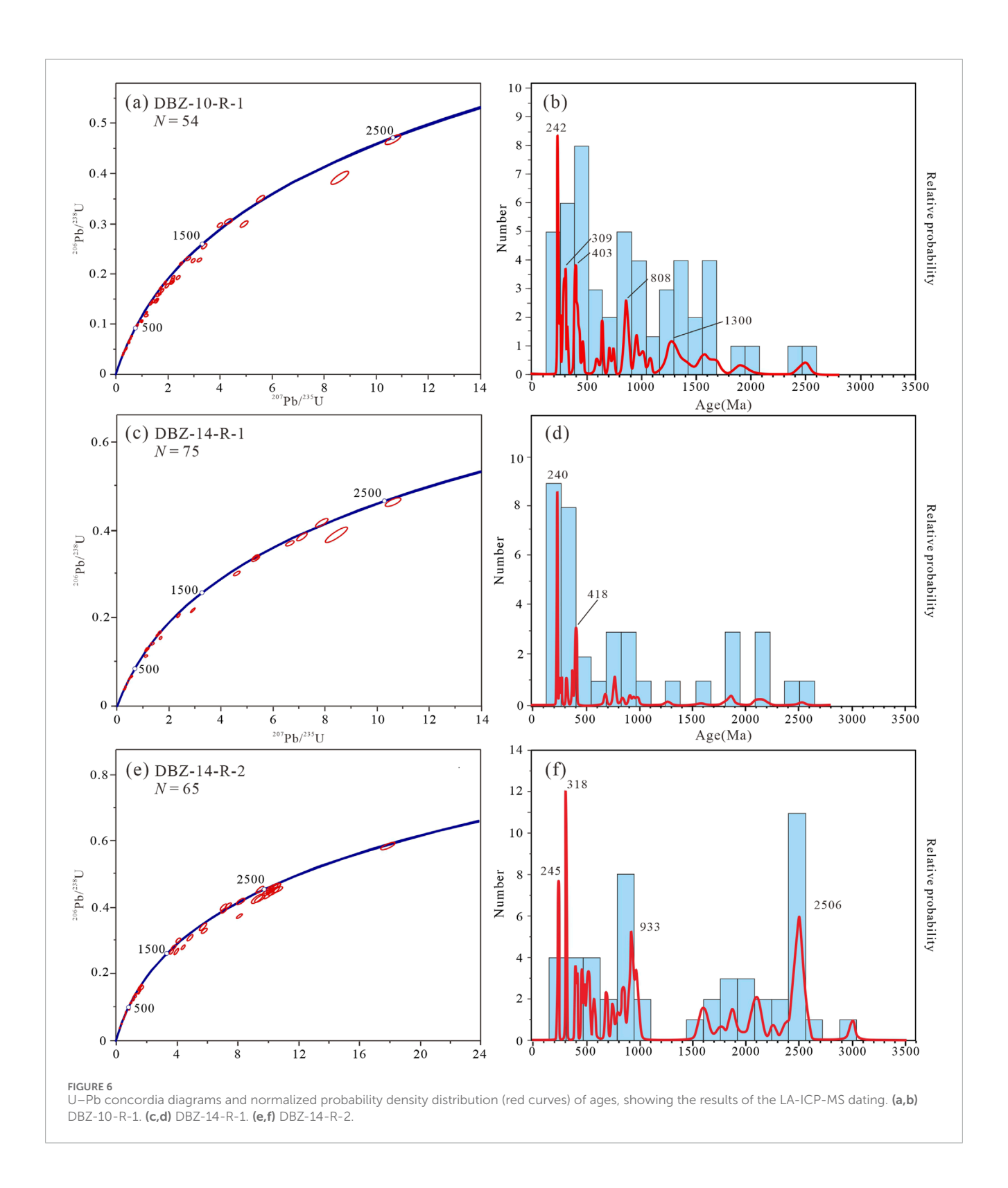
The detrital zircons predominantly show an age group of  $1000{\sim}800$  Ma, with  $\varepsilon$ Hf(t) values of  $-6.6{\sim}+11$ , and are present in samples DBZ-10-R-1 and DBZ-14-R-2. This corresponds to the extensively distributed magmatic rocks related to subduction in the margins surrounding Yangtze Block, such as  $900{\sim}720$  Ma mafic–ultramafic and felsic plutons in the Hannan region (Ao et al., 2019),  $820{\sim}810$  Ma felsic rocks in the Bikou region (Wu et al., 2019) and  $845{\sim}815$  Ma magmatic rocks in the Jiangnan orogenic belt with positive and negative  $\varepsilon_{\rm Hf}(t)$  values (Yao et al., 2019).

# 5.1.4 Ordovician to Devonian zircons (470~390 Ma)

The Ordovician to Devonian detrital zircons are only predominantly concentrated in the DBZ-10-R-1 and DBZ-14-R-1 samples yielding prominent age peak at  $\sim$ 410 Ma among the samples, and most zircons exhibit negative  $\epsilon$ Hf(t) values in previous study (Liu et al., 2023). In contrast to the distribution of adjacent rocks, the main source region correlates with the magmatic rocks in the NQOB. The early Paleozoic igneous rocks from this period were widely distributed in the NQOB (Wang et al., 2009). The  $\epsilon$ Hf(t) values of Ordovician to Devonian zircons in the samples are consistent with the contemporary magmatic rocks in the NQOB (Wang et al., 2020; Dong et al., 2022; Hu et al., 2022). Therefore, it is deduced the Ordovician to Devonian zircons were from the NQOB.

#### 5.1.5 Carboniferous zircons (330~290 Ma)

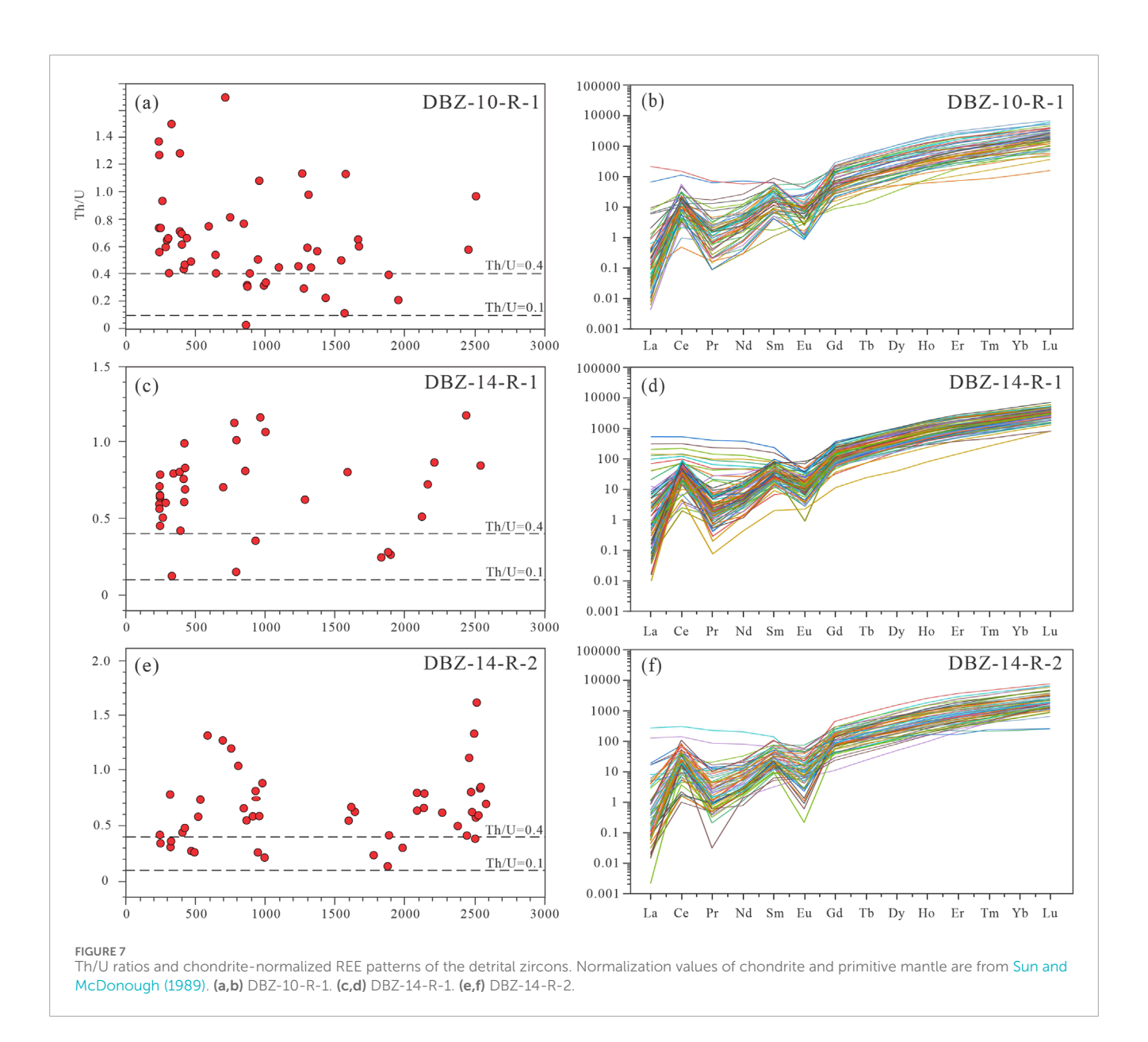
The Carboniferous detrital zircons are present in DBZ-10-R-1 and DBZ-14-R-1, which comprise a minor portion of



the total zircons. The contemporary granites are exclusively distributed in southwestern Fujian (Yu et al., 2012). Moreover, zircon populations of this age are well-documented in the underlying Late Permian clastic sequences in Fujian in the Cathaysian Block (Yu et al., 2012).

#### 5.1.6 Permian to triassic zircons (290~234 Ma)

The Permian to Triassic detrital zircons are remarkably observed in all three samples, especially with ages concentrated between 290~234 Ma yielding age peaks of ~245 Ma, with  $\epsilon$ Hf(t) values ranging from-10.9 to +4.5. In the AOB, massive felsic igneous



rocks are exposed in the range of 240~280 Ma, such as Xinanzhai granite at 251 Ma and Tongtiange leucogranite at 247.5 Ma, and have negative and positive  $\epsilon$ Hf(t) values (Liu et al., 2013; Liu et al., 2015). Besides, the early Mesozoic granites with the ages of 250~235 Ma are distributed in the SQOB. However, the  $\epsilon$ Hf(t) values of these rocks are negative (-8~0) and differ from the detrital zircons in studied samples. Therefore, the Permian to Triassic detrital zircons are mainly sourced from early Mesozoic rocks in the AOB.

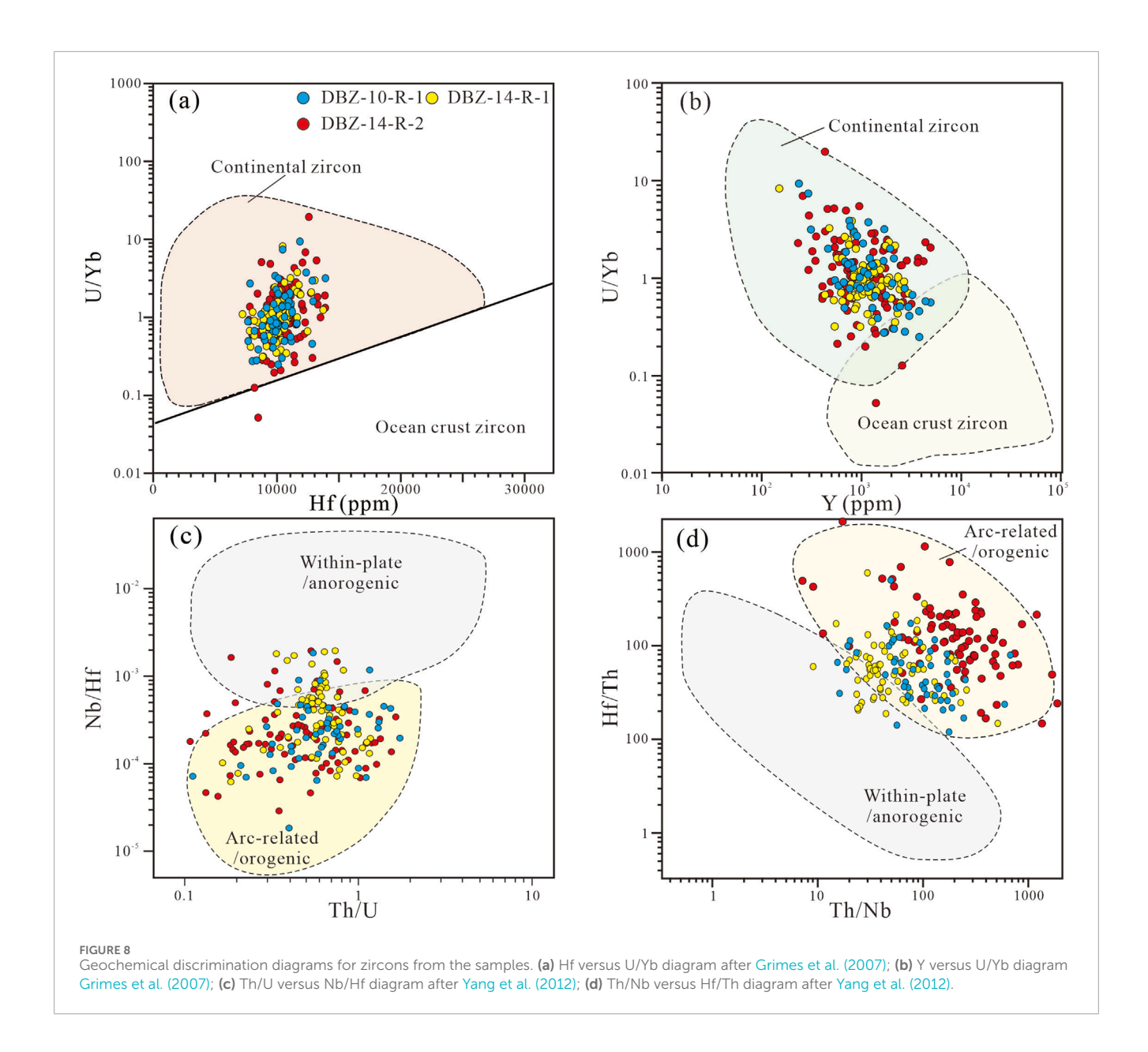
As discussed earlier, considering proximity and widespread distribution, the AOB, NQOB and Cathaysian Block are the primary source regions for the sample at middle part of the Leikoupo Formation, with a small quantity of original materials from the Yangtze Block. The potential main source region of the sample at the top is the Yangtze Block and AOB, and the secondary source region is the Cathaysian Block.

#### 5.2 Tectonic implications

The U-Pb age distribution characteristics can reflect the tectonic setting, and the samples of the Leikoupo Formation fall into a collisional background in the MDS plot (Figure 10), which implies that the Sichuan Basin, northwestern SCB, was primarily controlled by a collisional setting in the Middle Triassic. Meanwhile, it can infered that the Leikoupo Formation in the study region was formed in a continental margin tectonic setting during the middle Triassic period and the main detrital materials were derived from the coetaneous magmatic rocks.

# 5.2.1 Tectonic implications for the Qinling orogenic belt

The detrital zircon U-Pb age compositions of the Middle Triassic in the northern SCB, including Sichuan, Dangyang, Zigui

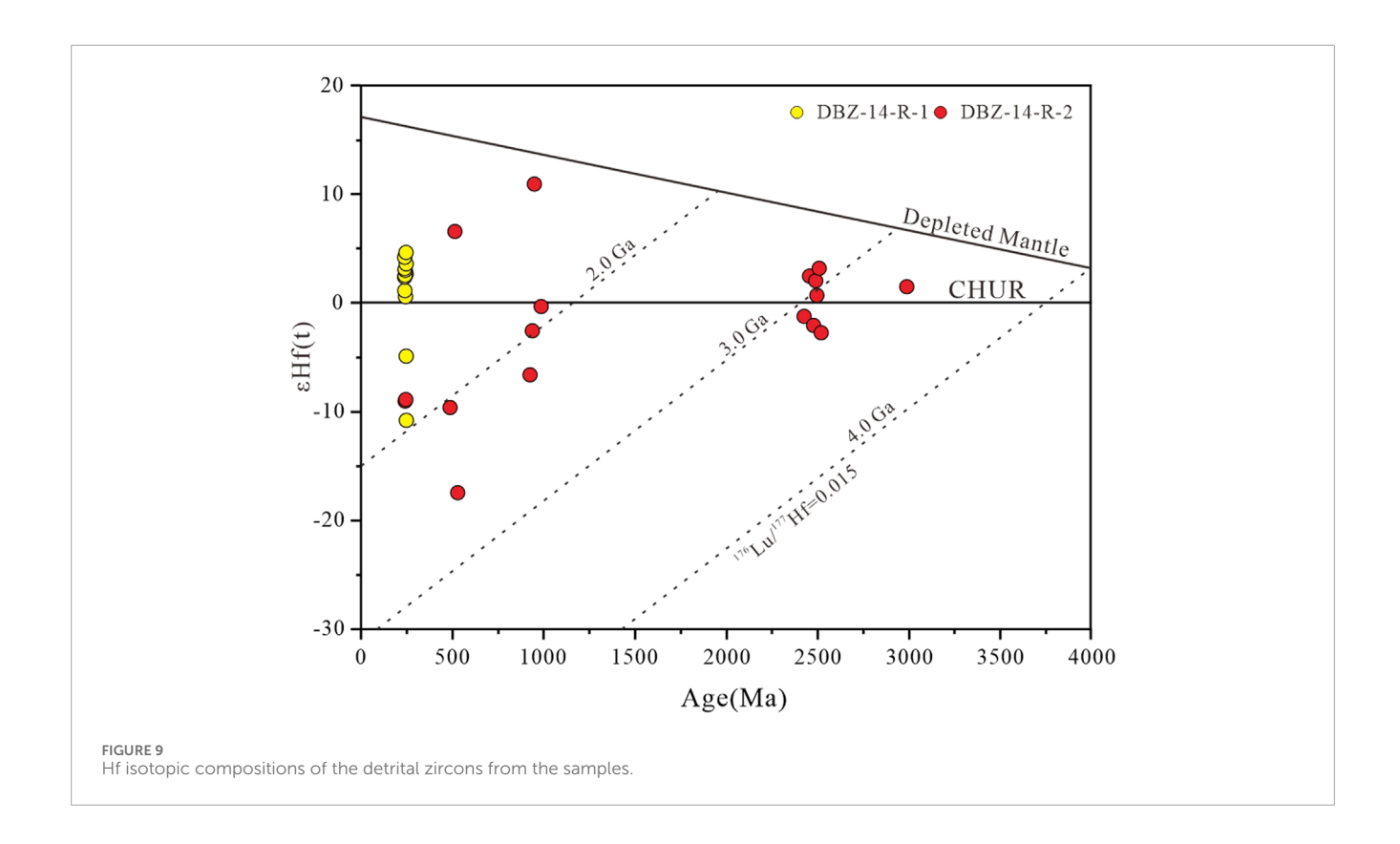


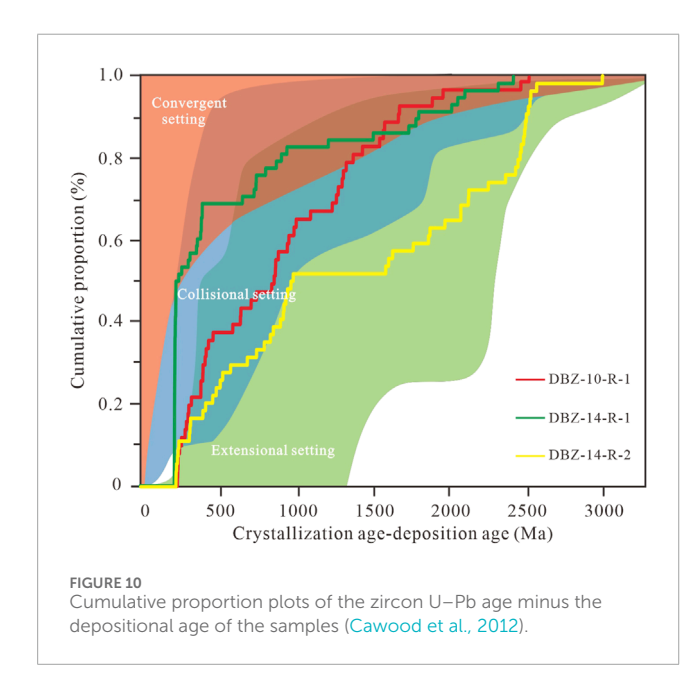
and Ningwu basins, form an main peak age of ~440 Ma (Chai, 2020; Ma, 2021; Li and Hu, 2022). These detrital zircons are sourced from the NQOB, which indicates this belt can provide most of detritus to the northern Yangtze Block and was in uplift state in the Middle Triassic. In addition, the Middle Triassic is not present in the NQOB, which indicates this belt has experienced a long-term denudation and was in a high paleotopography (Xu et al., 2023). The zircon geochronology indicates the Carboniferous-Early Triassic successions in the southern NCB received many detritus transported from the NQOB, which suggests the NQOB was in the uplift state since late Paleozoic (Peng et al., 2022; Yang et al., 2022). We infer that the Middle Triassic uplift of the NQOB was a continuation of the Paleozoic uplift (Dong et al., 2018; Yang et al., 2021; 2022). The provenance analysis indicates a large amount of debris can be transported from the NQOB

to the northern margin of the Yangtze Plate via the SQOB. In addition, the Early-Middle Triassic conglomerate and limestoneare sporadically exposed in the SQOB (Xu et al., 2023), which indicates that the depositional region was still remained during the Middle Triassic. Thus, the SQOB was not in the full-scale uplift during the Middle Triassic.

# 5.2.2 Tectonic implications for the Ailaoshan orogenic belt

The Paleozoic U-Pb age population of zircons in the Upper Permian on the eastern and western sides of the AOB show clear differences. The eastern region of the belt is featured by a main age peak at ~260 Ma and it is believed to originate from the Emeishan Large Igneous Province (Deng et al., 2020). In contrast, the western region





shows an age peak around ~420 Ma, likely sourced from the 450~400 Ma granites of the Changshan suture zone in northeastern Laos (Qiu et al., 2021). Besides, Late Permian siliceous rocks are exposed in the Gongka region in the AOB, which represents the deep-sea sediments. Thus, the Ailaoshan

Ocean still existed between the SCB and ICB during the late Permian, resulting in distinct sources of material for each block.

After the initial collision between the SCB and ICB, the AOB experienced tectonic uplift and was subjected to long-term erosion. The timing of the earliest fragmentary material from the AOB in the depositional area can accurately constrain the upper limit of timing of the orogenic belt's uplift. Provenance analysis indicates that Early Triassic strata in the depositional areas on the eastern and western sides of AOB contain ~245 Ma detrital zircons with an affinity with the AOB (Liu et al., 2022). This characteristic indicates AOB was in n a high paleotopography and experienced weathering and denudation (Liu et al., 2022). Additionally, the sedimentary age of the highest marine strata can provide an upper constraint on the timing of the uplift. Stratigraphic characteristics indicate a widespread absence of the Lower Triassic in the AOB, and the Middle Triassic strata are mainly argillaceous limestone, sandstone, and coal-bearing layers, which the Ailaoshan Ocean had already closed in the Early Triassic and that the AOB had entered a terrestrial evolution in the Middle Triassic (Yunnan Bureau of Geology and Mineral Resources, 1990). In the Early Triassic, EHf(t) values in the felsic igneous rocks and of Permian to Triassic detrital zircons in our samples are both negative and positive, which indicates a collision to post-collision tectonic background were dispersed throughout the AOB (Liu et al., 2022). Therefore, the forementioned provenance results and sedimentary characteristics suggest that the collisional amalgamation between the SCB and ICB, the Ailaoshan

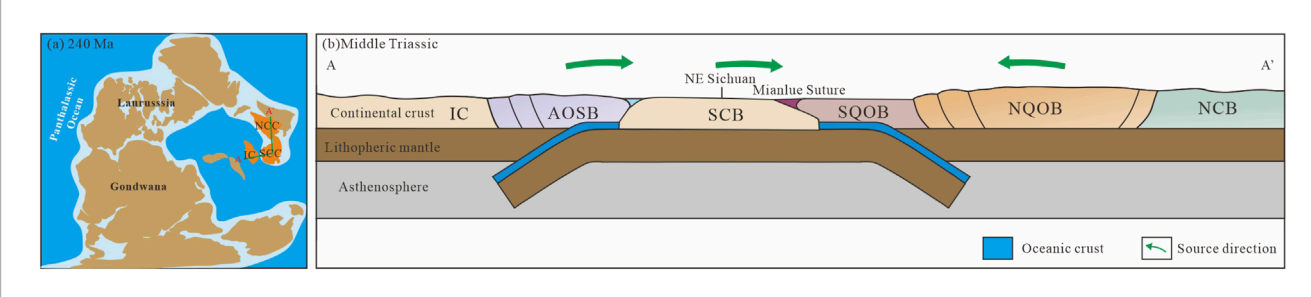


FIGURE 11

(a) Global paleogeographic reconstruction during the Middle Triassic (Huang et al., 2018); (b) Schematic model diagram of the tectonic uplift of the Ailaoshan and Qinling orogenic belts during the Middle Triassic. Abbreviation: SCB = South China Block; SQB = South Qinling orogenic belt; NQB = North Qinling orogenic belt; NCB = North China Block; AOB = Ailaoshan orogenic belt; ICB = Indochina Block.

Ocean closed in the early Early Triassic results in the uplift state of the AOB (Figure 11).

#### 6 Conclusion

- 1. The new date indicates that the original materials for the middle part of the Leikoupo Formation (Member-2) exhibiting major age group at 290~230 Ma, 330~290 Ma, 470~390 Ma, 900~840 Ma and 1400~1200 Ma, which are mainly originated from the Ailaoshan orogenic belt, North Qinling orogenic belt and the Cathaysian Block. The materials at the top (Member-3) exhibits major age group at 250~238 Ma, 330~300 Ma, 960~900 Ma and 2550~2450 Ma, and mainly derived from the Yangtze Block and Ailaoshan orogenic belt, and the secondary source region is the Cathaysian Block
- 2. Our study further reveals that the North Qinling orogenic belt was in the uplifted state during the middle Triassic, which was the extension of the Caledonian orogeny since the early Paleozoic. The Ailaoshan orogenic belt has experienced initial tectonic uplift in the early Triassic, which is related to the collisional amalgamation between the South China Block and Indochina Block.

## Data availability statement

The original contributions presented in the study are included in the article/Supplementary Material, further inquiries can be directed to the corresponding author.

#### **Author contributions**

TL: Writing – original draft. DZ: Writing – review and editing. YZ: Writing – review and editing. XL: Data curation, Writing – review and editing. LZ: Conceptualization, Writing – review and editing. LF: Formal Analysis, Writing – review and editing. CC: Project administration, Writing – review and editing. SF: Data curation, Writing – review and editing.

## **Funding**

The author(s) declare that financial support was received for the research and/or publication of this article. This research is supported by the National Key Research and Development Program of China (Project 2017YFC0602704).

### Conflict of interest

Authors TL, DZ, YZ, LZ, LF, and CC were employed by SINOPEC. Author XL was employed by PetroChina.

The remaining author declares that the research was conducted in the absence of any commercial or financial relationships that could be construed as a potential conflict of interest.

#### Generative Al statement

The author(s) declare that no Generative AI was used in the creation of this manuscript.

Any alternative text (alt text) provided alongside figures in this article has been generated by Frontiers with the support of artificial intelligence and reasonable efforts have been made to ensure accuracy, including review by the authors wherever possible. If you identify any issues, please contact us.

#### Publisher's note

All claims expressed in this article are solely those of the authors and do not necessarily represent those of their affiliated organizations, or those of the publisher, the editors and the reviewers. Any product that may be evaluated in this article, or claim that may be made by its manufacturer, is not guaranteed or endorsed by the publisher.

## Supplementary material

The Supplementary Material for this article can be found online at: https://www.frontiersin.org/articles/10.3389/feart.2025.1679009/full#supplementary-material

#### References

- Ao, W. H., Zhao, Y., Zhang, Y. K., Zhai, M. G., Zhang, H., Zhang, R. Y., et al. (2019). The Neoproterozoic magmatism in the northern margin of the yangtze block: insights from Neoproterozoic (950–706 ma) gabbroic-granitoid rocks of the Hannan complex. *Percambrian Res.* 333, 105442. doi:10.1016/j.precamres.2019.105442
- Cao, Y., Xu, Q., Zheng, J. F., Tan, X. C., Liu, M. L., Kershaw, S., et al. (2023). Two stages of Late Cretaceous to Neogene deformation of the huayingshan tectonic belt, eastern sichuan basin, SW China. *J. Asian Earth Sci.* 255, 105779. doi:10.1016/j.jseaes.2023.105779
- Caracciolo, L. (2020). Sediment generation and sediment routing systems from a quantitative provenance analysis perspective: review, application and future development. *Earth-Sci. Rev.* 209, 103226. doi:10.1016/j.earscirev.2020.103226
- Cawood, P. A., Hawkesworth, C. J., Dhuime, B., and Prave, T. (2012). Detrital zircon record and tectonic setting. *Geology* 40, 875–878. doi:10.1130/g32945.1
- Chai, R. (2020). Detrital records of the eastern qinling indosinian orogenic processes: sedimentology and sedimentary provenance analysis of the middle Triassic-Early Jurassic successions in zigui basin Ph.D. dissertation. Wuhan: China University of Geosciences, 1–131.
- Chen, Y. J. (2010). Indosinian tectonic setting, magmatism and metallogenesis in Qinling Orogen, central China. *Geol. China* 37, 854–865.
- Chen, K., Gao, S., Wu, Y. B., Guo, J. L., Hu, Z. C., Liu, Y. S., et al. (2013). 2.6-2.7 Ga crustal growth in yangtze craton, South China. *Precambrian Res.* 224, 472-490. doi:10.1016/j.precamres.2012.10.017
- Chen, Q., Sun, M., Zhao, G. C., Zhao, J. H., Zhu, W. L., Long, X. P., et al. (2019). Episodic crustal growth and reworking of the yudongzi terrane, South China: constraints from the Archean TTGs and potassic granites and Paleoproterozoic amphibolites. *Lithos* 326, 1–18. doi:10.1016/j.lithos.2018.12.005
- Deng, X. S., Yang, J. H., Cawood, P. A., Wang, X. C., Du, Y. S., Huang, Y., et al. (2020). Detrital record of late-stage silicic volcanism in the Emeishan large igneous province. *Gondwana Res.* 79, 197–208. doi:10.1016/j.gr.2019.09.015
- Dong, Y. P., and Santosh, M. (2016). Tectonic architecture and multiple orogeny of the Qinling Orogenic Belt, Central China. *Gondwana Res.* 29, 1–40. doi:10.1016/j.gr.2015.06.009
- Dong, Y. P., Zhang, G. W., Hauzenberger, C., Neubauer, F., Yang, Z., and Liu, X. M. (2011). Palaeozoic tectonics and evolutionary history of the Qinling orogen: evidence from geochemistry and geochronology of ophiolite and related volcanic rocks. *Lithos* 122, 39–56. doi:10.1016/j.lithos.2010.11.011
- Dong, Y. P., Liu, X. M., Neubauer, F., Zhang, G. W., Tao, N., Zhang, Y. G., et al. (2013). Timing of Paleozoic amalgamation between the North China and South China Blocks: evidence from detrital zircon U-Pb ages. *Tectonophysics* 586, 173–191. doi:10.1016/j.tecto.2012.11.018
- Dong, Y. P., Neubauer, F., Genser, J., Sun, S. S., Yang, Z., Zhang, F. F., et al. (2018). Timing of orogenic exhumation processes of the qinling orogen: evidence from 40Ar/39Ar dating. *Tectonics* 37, 4037–4067. doi:10.1029/2017tc004765
- Dong, Y. P., Shi, X. H., Sun, S. S., Sun, J. P., Hui, B., He, D. F., et al. (2022). Coevolution of the Cenozoic tectonics, geomorphology, environment and ecosystem in the Qinling Mountains and adjacent areas, Central China. *Geosy. Geoenviron.* 1, 100032. doi:10.1016/j.geogeo.2022.100032
- Fedo, C. M., Sircombe, K. N., and Rainbird, R. H. (2003). Detrital zircon analysis of the sedimentary record. *Rev. Mineral. Geochem.* 53, 277–303. doi:10.2113/0530277
- Galindo-Ruiz, J., Ramirez-Montoya, E., Madhavaraju, J., Grijalva-Noriega, F. J., Solari, L., Monreal, R., et al. (2025). Influence of Triassic and Jurassic arc magmatism in Lower Jurassic Sierra de Santa Rosa Formation, northwestern México: constraints from geochemistry and U-Pb geochronology. *Pet. Geol.* 171, 107168. doi:10.1016/j.marpetgeo.2024.107168
- Gehrels, G. (2014). Detrital zircon U-Pb geochronology applied to tectonics. *Rev. Earth Planet. Sci.* 42, 127–149. doi:10.1146/annurev-earth-050212-124012
- González-León, C. M., Madhavaraju, J., Ramírez Montoya, E., Solari, L. A., Villanueva-Amadoz, U., Monreal, R., et al. (2020). Stratigraphy, detrital zircon geochronology and provenance of the morita formation (bisbee group) in northeastern Sonora, Mexico. *J. S. Am. Earth Sci.* 103, 102761. doi:10.1016/j.jsames.2020.102761
- Grimes, C. B., John, B. E., Kelemen, P. B., Mazdab, F. K., Wooden, J. L., Cheadle, M. J., et al. (2007). Trace element chemistry of zircons from oceanic crust: a method for distinguishing detrital zircon provenance. *Geology* 35, 643–646. doi:10.1130/g23603a.1
- Guo, J. L., Wu, Y. B., Gao, S., Jin, Z. M., Zong, K., Hu, Z. C., et al. (2015). Episodic Paleoarchean-Paleoproterozoic (3.3–2.0 Ga) granitoid magmatism in Yangtze Craton, South China: implications for late Archean tectonics. *Tectonics* 270, 246–266. doi:10.1016/j.precamres.2015.09.007
- He, D. F., Li, Y. Q., Huang, H. Y., Zhang, J., Lu, R. Q., and Li, D. (2020). Formation and evolution of polycyclic superimposed basin and petroleum accumulation in Sichuan. Beijing: Science Press, 1–569.
- Hou, K. J., Li, Y. H., Zou, T. R., Qu, X. M., Shi, Y. R., and Xie, G. Q. (2007). Later ablation-MC-ICP-MS technique for Hf isotope microanalysis of zircon and its geological application. *Acta Petrol. Sin.*, 2595–2604.

- Hu, J., Liu, X. C., Chen, L. Y., Qu, W., Li, H. K., and Geng, J. Z. (2013). A ~2.5 Ga magmatic event at the northern margin of the Yangtze craton: evidence from U-Pb dating and hf isotope analysis of zircons from the douling complex in the South Qinling orogen. *Chin. Sci. Bull.* 58, 3564–3579. doi:10.1007/s11434-013-5904-1
- Hu, P., Zeng, W., Xiong, J. L., Liu, X., Li, G. Y., and Wang, J. Y. (2022). Genesis of wuduoshan I-S type granite and the constraints on the early Paleozoic rectonic evolution of the Northern Qinling: evidence from zircon U-Pb age, geochemistry and sr-nd-hf isotopes. *Golo. Bull. China* 41, 810–823. doi:10.12097/j.issn.1671-2552.2022.05.007
- Huang, B. C., Yan, Y. G., Piper, J. D. A., Zhang, D. H., Yi, Z. Y., Yu, S., et al. (2018). Paleomagnetic constraints on the paleogeography of the East Asian blocks during late Paleozoic and early Mesozoic times. *Earth Sci. Rev.* 186, 8–36. doi:10.1016/j.earscirev.2018.02.004
- Hui, B., Dong, Y. P., Cheng, C., Long, X. P., Liu, X. M., Yang, Z., et al. (2017). Zircon U-Pb chronology, hf isotope analysis and whole-rock geochemistry for the Neoarchean-Paleoproterozoic Yudongzi complex, northwestern margin of the Yangtze craton, China. *Precambrian Res.* 301, 65–85. doi:10.1016/j.precamres.2017.09.003
- Hui, B., Dong, Y. P., Zhang, F. F., Sun, S. S., Liu, X. M., Cheng, C., et al. (2019). Geochronology and geochemistry of *ca.* 2.48 Ga granitoid gneisses from the Yudongzi Complexin the north-western Yangtze Block, China. *Geol. J.* 54, 879–896. doi:10.1002/gj.3396
- Jian, X., Guan, P., Fu, L., Zhang, W., Shen, X. T., Fu, H. J., et al. (2024). Detrital zircon geochronology and provenance of Cenozoic deposits in the Qaidam Basin, Northern Tibetan plateau: an overview with new data, implications and perspectives. *Mar. Petrol. Geol.* 159, 106566. doi:10.1016/j.marpetgeo.2023.106566
- Li, C., and Hu, X. M. (2022). The earliest denudation record of the Dabie Orogenic Belt evidenced from the middle Triassic Huangmaqing formation in the ningwu Basin. *Geol. J. China Univ.* 28, 527–538.
- Liu, Y. S., Gao, S., Hu, Z. C., Gao, C. G., Zong, K. Q., and Wang, D. B. (2010). Continental and Oceanic crust recycling-induced melt-peridotite interactions in the trans-north China orogen: U–Pb dating, Hf isotopes and trace elements in zircons from mantle xenoliths. *J. Petrol.* 51, 537–571. doi:10.1093/petrology/egp082
- Liu, H. C., Wang, Y. J., Cai, Y. F., Ma, L. Y., Xing, X. W., and Fan, W. M. (2013). Zircon U-Pb geochronology and Hf isotopic compositions of the Xin'anzhai granite along the ailaoshan tectonic zone in west Yunnan province. *Geotect. Metal.* 37, 87–98. doi:10.3969/j.issn.1001-1552.2013.01.010
- Liu, H. C., Wang, Y. J., Cawood, P. A., Fan, W., Cai, Y., and Xing, X. (2015). Record of tethyan ocean closure and Indosinian collision along the ailaoshan suture zone (SW China). *Gondwana Res.* 27, 1292–1306. doi:10.1016/j.gr.2013.12.013
- Liu, B. B., Peng, T. B., Fan, W. M., Dong, X. H., Peng, S. Z., Wu, L. M., et al. (2022). Timing of the ailaoshan paleo-tethys ocean closure and the in dosinian orogeny initiation: constraints from the detrital zircon U-Pb geochronology and Hf isotopes of the middle-upper Triassic strata. *Geotect. Metallogenia* 46, 132–192.
- Liu, T. J., Wang, X. L., Wang, Z. T., Santosh, M., Liu, X. F., Ju, P. C., et al. (2023). Depositional response to the emeishan mantle plume: evidence from the eastern sichuan Basin, South China. *Int. Geol. Rev.* 65, 3311–3328. doi:10.1080/00206814.2023.2185821
- Ma, Q. L. (2021). Mesozoic sedimentary records in the northern margin of the middle Yangtze: the successive response to the collision–uplift process of the qinling orogenic Belt Ph.D. dissertation. Wuhan: China University of Geosciences, 1–273.
- Madhavaraju, J., Saucedo-Samaniego, J. C., Löser, H., Espinoza-Maldonado, I. C., Solari, L., Monreal, R., et al. (2019). Detrital zircon record of Mesozoic volcanic arcs in the Lower Cretaceous Mural Limestone, northwestern Mexico. *Geol. J.* 54, 2621–2645. doi:10.1002/gj.3315
- Pei, X. Z., Li, H. M., Zhang, G. G., Zhang, W. J., and Wang, Q. Q. (1997). Sm-Nd ages and geological significance of amphibolites of the wudang group complex on the southern side of the Shangdan fault zone in the east qinling Mountains. *Geol. Bull. China* 16, 38–42.
- Peng, Y. Q., Yang, W. T., Zhang, H. Y., and Fang, T. (2022). Provenance characteristics and sedimentary-tectonic evolution of the North China Basin in the Triassic: indications from detrital zircon ages. *Acta Sedi*. 40, 1228–1249.
- Qiu, X., Wang, Y. J., Qian, X., and Zhang, Y. Z. (2021). Detrital Zircon U-Pb geochronology and geochemical characteristics of Permian sandstones in NW Laos and its tectonic implications. *Earth Sci.* 46, 3910–3925.
- Ramírez-Montoya, E., Madhavaraju, J., González-León, C. M., Armstrong-Altrin, J. S., and Monreal, R. (2022). "Detrital zircon geochemistry in the morita formation, Northern Sonora, Mexico: implications for origin and source rock type," in *Geochemical treasures and petrogenetic processes*. Editors J. A. Armstrong-Altrin, K. Pandarinath, and S. Verma, 315–350.
- Ramirez-Montoya, E., Madhavaraju, J., Monreal, R., and Solari, L. (2025). Depositional age and provenance of Triassic sedimentary succession from Northwestern México: evidence from petrography and detrital zircon U–Pb geochronology. *J. Palaeogeog.* 14, 370–390. doi:10.1016/j.jop.2025.01.001

Ren, J. S., Zhu, J. B., Li, C., and Liu, R. Y. (2019). Is the qinling orogen an indosinian collisional orogenic belt? *Earth Sci.* 44, 1476–1486.

- Siebel, W., Schmitt, A. K., Danisík, M., Chen, F. K., Meier, S., Weiss, S., et al. (2009). Prolonged mantle residence of zircon xenocrysts from the western Eger rift. *Nat. Geosci.* 2. 886–890.
- Sun, S. S., and McDonough, W. F. (1989). Chemical and isotopic systematics of oceanic basalts: implications for mantle composition and processes. *Geo. Soc. Lond. Spec. Pub.* 42, 313–345. doi:10.1144/gsl.sp.1989.042.01.19
- Sun, J. J., Shu, L. S., Santosh, M., and Wang, L. S. (2018). Precambrian crustal evolution of the central Jiangnan orogen (South China): evidence from detrital zircon U-Pb ages and Hf isotopic compositions of Neoproterozoic metasedimentary rocks. *Precambr. Res.* 318, 1–24. doi:10.1016/j.precamres.2018.09.008
- Terentiev, R. A., and Santosh, M. (2016). Detrital zircon geochronology and geochemistry of metasediments from the vorontsovka terrane: implications for microcontinent tectonics. *Int. Geol. Rev.* 58, 1108–1126. doi:10.1080/00206814.2016.1147386
- Wang, T., Wang, X. X., Tian, W., Zhang, C. L., Li, W. P., and Li, S. (2009). North qinling Paleozoic granite associations and their variation in space and time: implications for orogenic processes in the orogens of central China. *Sci. China-Earth Sci.* 52, 1359–1384. doi:10.1007/s11430-009-0129-5
- Wang, J. B., Li, T., Zhang, Y., and Li, W. H. (2020). Water-flux melting of amphibolite in Paleozoic leucogranite from the north qinling, central China: implication for post collisional setting. *J. Earth Sci.* 31, 867–874. doi:10.1007/s12583-020-1335-5
- Wang, Y. T., Sun, G. Q., Bo, S. S., Fu, S., Cruset, D., Martín-Martín, J. D., et al. (2023). Detrital zircon U-Pb dating and geochemistry of the Paleogene-Neogene sediments in the qaidam basin (China): implications for provenance and tectonics. *Glob. Planet. Change* 228, 104202. doi:10.1016/j.gloplacha.2023.104202
- Wu, Y. B., Zhou, G. Y., Gao, S., Liu, X. C., Qin, Z. W., Wang, H., et al. (2014). Petrogenesis of Neoarchean TTG rocks in the Yangtze Craton and its implication for the formation of Archean TTGs. *Precambrian Res.* 254, 73–86. doi:10.1016/j.precamres.2014.08.004
- Wu, T., Wang, X. C., Li, W. X., Wilde, S. A., and Tian, L. Y. (2019). Petrogenesis of the ca. 820–810 Ma felsic volcanic rocks in the Bikou group: implications for the tectonic setting of the Western margin of the yangtze Block. *Percambrian Res.* 331, 105370. doi:10.1016/j.precamres.2019.105370
- Xu, Y. H., He, D. F., Cheng, X., and Guo, J. Y. (2023). Discussion on evolution and formation mechanisms of Triassic nanzhao basin in North Qinling tectonic belt. *Chin. J. Geol.* 58, 214–225. doi:10.12017/dzkx.2023.014
- Yang, L., Chen, F. K., Yang, Y. Z., Li, S. Q., and Zhu, X. Y. (2010). Zircon U-Pb ages of the Qinling Group in Danfeng area: recording Mesoproterozoic and Neoproterozoic

- magmatism and early Paleozoic metamorphism in the North Qinling terrain. Acta Petrol, 26, 589–1603.
- Yang, J. H., Cawood, P. A., Du, Y. S., Huang, H., Huang, H. W., and Tao, P. (2012). Large igneous province and magmatic arc sourced Permian–Triassic volcanogenic sediments in China. Sediment. Geol. 261–262, 120–131. doi:10.1016/j.sedgeo.2012.03.018
- Yang, W. T., Peng, S. Y., Wang, M., Zhang, H. Y., and Zhang, H. Y. (2021). Provenance of upper Permian-Triassic sediments in the south of North China: implications for the Qinling orogeny and basin evolution. *Sediment. Geol.* 424, 106002. doi:10.1016/j.sedgeo.2021.106002
- Yang, W. T., Fang, T., Wang, Y. P., and Sha, H. (2022). Late Paleozoic tectonic evolution of the qinling orogenic belt: constraints of detrital zircon U-Pb ages from the Southern Margin of North China block. *Minerals* 12, 864. doi:10.3390/min12070864
- Yao, J. L., Shu, L. S., and Santosh, M. (2011). Detrital zircon U-Pb geochronology, Hf-isotopes and geochemistry—New clues for the Precambrian crustal evolution of cathaysia block, South China. *Gondwana Res.* 20, 553–567. doi:10.1016/j.gr.2011.
- Yao, J. L., Cawood, P. A., Shu, L. S., and Zhao, G. C. (2019). Jiangnan orogen, South China: a similar to 970-820 Ma rodinia margin accretionary belt. *Earth-Sci. Rev.*, 196.
- Yu, J. H., Liu, Q., Hu, X. M., Wang, Q., and O'Reilly, S. Y. (2012). Late Paleozoic magmatism in South China: oceanic subduction or intracontinental orogeny? *Chin. Sci. Bull.* 58, 788–795. doi:10.1007/s11434-012-5376-8
- Yunnan Bureau of Geology and Mineral Resources (YNGMR) (1990). Regional geology of Yunnan Province. Beijing: Geological Publishing House, 45–201.
- Zhang, G. W., Meng, Q. R., Yu, Z. P., Sun, Y., Zhou, D. W., and Guo, A. L. (1996). Orogenesis and dynamics of Qinling orogen. *Sci. China-Earth Sci.* 26, 193–200.
- Zhang, G. W., Zhang, B. R., and Yuan, X. C. (2001). Qinling orogenic belt and Continental dynamics. Beijing: Science Press, 1–855.
- Zhao, G. C., and Cawood, P. A. (2012). Precambrian geology of China. *Precambrian Res.* 222, 13–54. doi:10.1016/j.precamres.2012.09.017
- Zheng, J. P., Griffin, W. L., O'Reilly, S. Y., Zhang, M., Pearson, N., and Pan, Y. M. (2006). Widespread Archean basement beneath the yangtze craton. *Geology* 34, 417–420. doi:10.1130/g22282.1
- Zhong, D. (1998). The paleo-Tethyan orogenic belts, Western Yunnan and sichuan provinces. Beijing: Science Press, 1–231.
- Zhou, G. Y., Wu, Y. B., Li, L., Zhang, W. X., Zheng, J. P., Wang, H., et al. (2018). Identification of ca. 2.65 Ga TTGs in the yudongzi complex and its implications for the early evolution of the yangtze block. *Precambrian Res.* 254, 240–263. doi:10.1016/j.precamres.2018.06.011